

**BALKANTRIB'05**  
**5<sup>th</sup> INTERNATIONAL CONFERENCE ON TRIBOLOGY**  
**JUNE.15-18. 2005**  
**Kragujevac, Serbia and Montenegro**

---

---

**DEVICES FOR TRIBOTESTS AT MICRO/NANO SCALE**

N.K. MYSHKIN

*Metal-Polymer Research Institute, Kirova st. 32A, 246050 Gomel, Belarus, e-mail:*

**Abstract**

*There is a scale factor affecting the data for macro and micro systems, so the test equipment should be designed with account of this factor. We describe such equipment including contact adhesion meter, rotary and reciprocating microtribometers. We investigated the adhesion forces between the ball probes and materials used in microsystems: silicon plates, steel plates, thin coatings, and self-assembled monolayers on silicon plates. Silicon, quartz and steel balls were used as probing samples. Advantages and drawbacks of instruments are discussed.*

**Keywords:** *Microtribology, adhesion, friction, testing equipment, self-assembled monolayers*

## 1 INTRODUCTION

Modern high-technology systems operate in micro- and nanometer scale because their components are produced with very smooth surfaces [1].

Common macroscopic tribological principles cannot be applied directly to microsystems mainly due to influence of different factors on friction and wear in macro and microscale.

Surface forces and adhesion are the dominant factors affecting the tribological behaviour at microscale. For example, it is known that operation of MEMS (micro-electro-mechanical systems) depends mainly on adhesion of parts in contact [2].

Much of research in microtribology is done with atomic force microscope (AFM), lateral force microscope (LFM), and surface force apparatus (SFA). But these instruments provide data, which cannot be directly applied to real engineering systems and bridging the gap between macro and microtribology calls for use the adequate test equipment.

We tried to design such equipment and apply to some objects, e.g. self-assembled monolayers often used in microsystems.

## 2. EXPERIMENTAL EQUIPMENT

Usually the components of micro/nano systems operate under light loads (order of a few  $\mu\text{N}$ ), that means in the range of values of surface forces. In order to simulate their operation efficiently we need to use the same range of loads.

### 1.1 Contact Adhesion Meter

The range of surface forces between the macroscopic bodies can be compared with the sensitivity of an accurate analytical balance. But the measurements should be carried out at a very small speed impossible for common balance. Derjagin et al. proposed to solve the problem [3] by applying the principle of a feedback balance.

In our case we have chosen the design of a vertical torsion balance with negative feedback. This design eliminates the problems with balancing and errors caused by friction in the balance support.

The measuring unit of the contact adhesion meter (CAM) is a vertically disposed frame 1 (Figure 1) suspended on string 2. One arm of the frame carries holder 3 of a probing specimen (ball). Another arm of the frame carries movable coil 4 of a measuring electromagnet connected with a highly stable current source. Mirror 5 is fastened to the frame. It reflects the beam of

laser 6, which then passes expander of optical base 7 and impinges photodetector 8. When force starts to act between the specimens frame 1 with mirror 5 turns thus changing the light flux impinging photodetector 8. The signal of the photodetector forms a feedback signal, which varies current in coil 9 until the frame has turned to its initial position. So, any variation in the forces acting between the specimens is compensated by a corresponding current variation that remains the frame stationary in measuring process. Current in coil 9 is calibrated. So, the forces acting between specimen 10 and the ball can be measured.

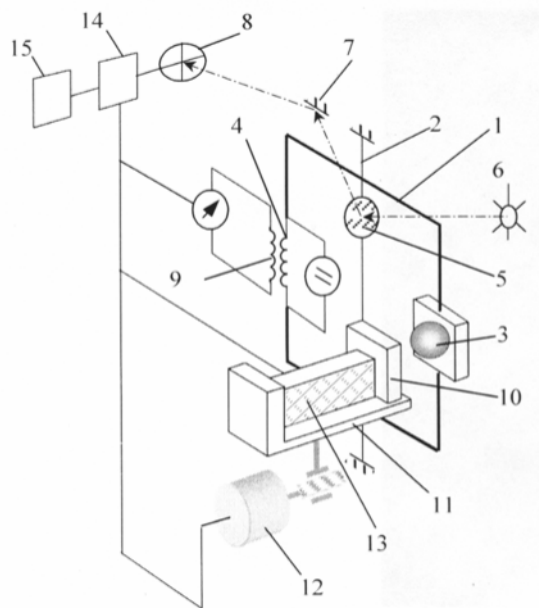


**Figure 1:** *Principal scheme of adhesion meter*

Specimen under testing 10 is placed on table 11 equipped with a system of rough positioning driven by stepping motor 12 and with a system of fine positioning driven by piezodrive 13.

Initially the specimen and the ball are removed to a distance at which they do not influence each other. Piezodrive 13 is stretched. In this position current passing measuring electromagnet 9 is assumed to correspond to zero force between the specimens. Then specimen 10 is approached to the probing specimen by stepping motor 12 until a preset initial contact load is attained. Depending on the aim of the experiment the measuring cycle can start either on reaching the required contact load or after a certain period of time.

Adhesion is measured when moving off specimen 10 with piezodrive 13 by plotting the

dependence of the force acting between the specimens on the distance. In the process of moving off the force varies and this variation is compensated by current in coil 9 that provides a stationary position of the frame. When a preset distance is reached the measurement is performed in reverse order, namely when approaching the specimen to the probe. As a result, two dependencies are obtained characterizing the force of interaction when moving off and approaching the specimen to the ball.

To protect the apparatus from vibrations and to retain a constant temperature it was mounted on a table with a magnetic-fluid damper. The table is suspended on strings into a wooden case with a sound-proof lagging made of cellular polystyrene and metallized polyethylene film.

A programmable analog-digital signal processor 14 performs control of the measuring process.

The test data are processed and operation modes are set by software operating in Windows by the signal processor through a parallel port of PC 15. Basic characteristics of the apparatus are listed in the Table 1.

**Table 1: Characteristics of contact adhesion meter**

Measured forces, mN	0.01– 10
Sample displacements, nm	10 – 10000
Sample size, mm	20×20×5
Probe size (ball type), mm	0.2 – 5

## 1.2 Reciprocating Precision Tribometer

We developed a special tribometer with a precision reciprocating motion. It has a controlled normal load of 10 mN – 1 N and sliding velocity of 0.1 – 10 mm/s. We selected a sphere-plane scheme, which allows us to calculate most accurately the contact area and pressure as well as to exclude inevitable influence of indenter and plate slopes on the contact geometry. The ball diameter is chosen within 1 – 5 mm according to the required contact pressure. To provide the efficient monitoring of the specimen surface layers the tribometer is equipped with an acoustic emission (AE) recording unit. The specimen testing process is fully automatic.

The main schematic of the microtribometer is shown in Figure 2.

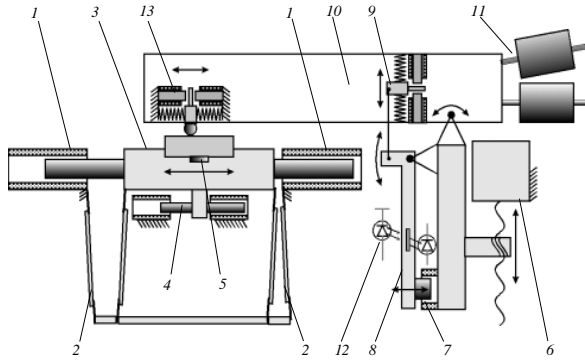


**Figure 2:** Precision tribometer scheme: 1 — drive electromagnets; 2 — flexible guides; 3 — holder table for specimens; 4 — position transducer; 5 — acoustic emission transducer; 6 — stepping drive; 7 — electromagnet of loading unit; 8 — lever; 9 — loading transducer; 10 — head; 11 — balancing weights; 12 — optocoupler; 13 — friction force transducer

The holder of the plate specimen 3 is connected to the anchors of drive electromagnets 1 and in testing it reciprocates in the horizontal plane. An elastic suspension is used as movement guides 2 which allow us to avoid jump-wise displacement at low sliding velocities, noise and vibration being characteristic of sliding and rolling guides. Owing to the symmetrical design of the guides the normal displacement of the specimen is absent during the holder movement.

Usage of the contactless drive is minimizing the mechanical noise and vibration that negatively affected the measurement of low friction forces. The electromagnetic drive in combination with the flexible guides makes possible to move specimens within the required velocity range with a stroke length from 0.1 to 10 mm. In addition, the electromagnetic drive is helpful in realization of different modes of specimen movement.

It is known that the validity of the tribotest results is directly related to the stiffness of displacement control and friction force measuring system. Regardless the drive design for moving the specimens (piezoelectric or electromagnet) the occurrence of the friction force in ball-plate interaction influences the uniformity of the drive movement, which results in errors in the friction force measurement. In case of including displacement transducers 4 into the feedback system the influence of the friction force on the drive movement parameters can be partially compensated. It is found

experimentally that the use of feedback by the specimen position results in drive stiffness increase by an order of magnitude and even more at invariable parameters of the electromagnets and suspension rigidity. A contactless unit consisting of two coils fixed to the stationary base and a moving core mechanically attached to the drive elements is used as a transducer of the specimen holder position. The coil windings are included into the half-bridge scheme that records the core position changing the coil inductance. The given scheme for measuring displacements is less subjected to the influence of environment in contrast to the capacity measurement systems used in SFA [4]. The disadvantage of the inductance transducers is related to their lower sensitivity compared to capacity ones as well as undesirable influence of the alternating magnetic field excited in the coils on the measurement data.

The normal load of the indenter on the specimen is set and kept constant in testing by an electromagnetic unit with feedback. The traction force of electromagnet 7 (Figure 2) is transmitted with lever 8 through the load transducer 9 to oscillating head 10. The initial balancing of the head is made with weights 11. Angular position of the head is monitored with optic couple 12 whose signal depends on the slope angle of lever 8. Electromagnet 7 and load transducer 9 form a circuit with feedback owing to which the normal load is kept constant regardless the normal displacement of the head due to errors in producing and setting the specimen. Stepping drive 6 is used for moving the indenter to the specimen surface as well as its separation from the surface after testing.

### 1.3 Rotary/Reciprocating Microtribometer

The general scheme of rotary and reciprocating microtribometer is presented in Figure 3.

The base plate 1 is used for support of the tester parts and electric boards with power supply unit. The string suspension 8 supports the loading system. The laser system 9 is used for measuring angle position of the loading system, which depends on value of friction force. The stage 6 is rotated by low speed revolution motor 4. It can be replaced by a reciprocating stage providing the stroke to 5 mm. The device is equipped by system of horizontal positioning 2 for changing the radius of wear track.

The control electric circuit based on digital signal processor is connected to the PC by COM port. When the normal load is applied to the ball the friction force causes rotation of the loading system suspended by vertical string. The mirror fixed on string suspension reflects the laser beam. The beam spot position is detected by photodetector. The position-sensitive detector and electromagnetic system assembled with string suspension are connected with feedback circuit to compensate the friction force.

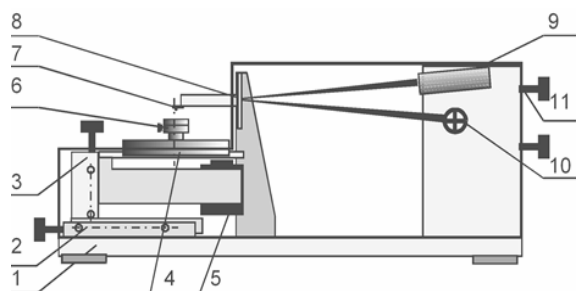


**Figure 4:** General scheme of rotary/reciprocating microtribometer: 1 – base plate; 2 – horizontal positioning plate; 3 – system of vertical positioning; 4 – rotary or linear electromagnetic motor; 5 – electromagnet; 6 – sample stage; 7 – ball holder; 8 – spring suspension; 9 – laser; 10 – four-quadrant photo detector; 11 – tuning screws.

The loading system consists of permanent magnet, steel ring, winding, holder of ball specimen and balancing weight. The loading force is caused by the interaction between electrical current passed through the winding and magnetic field of the permanent magnet. The magnitude of produced force is independent from the angular position of the holder. It means that the magnitude of load applied by the loading system is independent from the topography effect and small tilt angles of the specimen. Technical specification of the rotary/reciprocating microtribometer is listed in the Table 2.

**Table 2: Characteristics of microtribometer**

Normal load, mN	0.01 – 10
Sliding speed, mm/s	0.06 - 4
Radius of wear track, mm	to 10
Ball size, mm	0.2 – 4

## 2 TEST SAMPLES

We measured the adhesion and friction forces of thin coatings and different self-assembled monolayers. Chemical structure and method of deposition is described elsewhere [5]. For inorganic DDPO<sub>4</sub> and ODPO<sub>4</sub> SAMs the initial silicon substrates were covered by Ti or TiO<sub>x</sub> sublayers. Polymer SAMs were deposited on silicon substrates. Basic characteristics of the specimens being tested are listed in Table 3.

**Table 3: Basic characteristics of the specimens**

Sample	Description
Si	Substrate
Ti	Ti coating (100 nm) on Si substrate
TiO <sub>x</sub>	TiO <sub>x</sub> coating (20 nm) on Si substrate
DLC	Diamond like carbon (~200 nm) on Si substrate
Ti-ODPO <sub>4</sub>	Octadecylphosphoric acid ester (2.2 nm) on Ti covered Si substrate
TiO <sub>x</sub> -ODPO <sub>4</sub>	Octadecylphosphoric acid ester on TiO <sub>x</sub> covered Si substrate
TiO <sub>x</sub> -DDPO <sub>4</sub>	dodecylphosphoric acid ester on TiO <sub>x</sub> covered Si substrate
OTS	Octadecyltrichlorsilane (2.6 nm) on Si substrate
SEBS	Poly[styrene – b - (ethylene-co-butylene) - b- styrene] (1.67 nm) on Si substrate
Epoxilane	SAM (~1 nm) with epoxy surface groups on Si substrate

All tests were carried out at a temperature 18±2°C, atmospheric pressure 740±15 mm Hg and relative humidity 60-70%.

## 3 TEST RESULTS AND DISCUSSION

### 3.1 Measurement of adhesion

Typical dependence of adhesion force during approaching of various balls to the investigated samples obtained by contact adhesion meter is shown on the Figure 5. It shows two experimental dependences of force interaction

on the distance obtained with different probes and samples. The curves are obtained in approaching of solids. They illustrate the kinetics of force interaction between the contact surfaces.

We used two spherical indenters as the test counterbodies: a silicon ball (diameter 2 mm), titanium ball (diameter 3 mm).

Curve 1 corresponds to interaction between the silicon ball and the silicon substrate coated with  $TiO_x$  on which a monomolecular layer of  $ODPO_4$  is deposited. Curve 2 describes interaction between the titanium ball and the silicon plate.

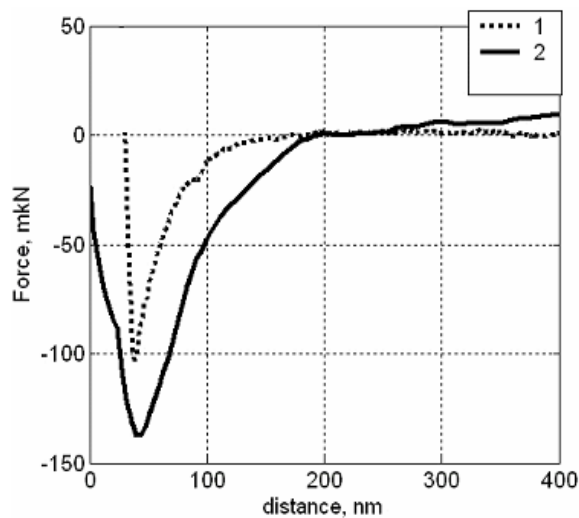


**Figure 5:** Experimental dependence force – distance: 1 – interaction of silicon ball and  $Si+TiO_x+ODPO_4$ , 2 – interaction between titanium ball and silicon plate.

Pattern of experimental data shows that irrespective of the nature of contacting solids the force-distance curves have similar shapes. Starting from some distance the attraction force between solids monotonously grows up, and then the direction of the force reverses. At this stage attraction stops to dominate and the phenomenon of repulsion occurs which grows much faster in comparison with attraction.

For calculation of specific surface energy  $\gamma$  of samples it is necessary to know the same characteristic for probes. For a silicon ball it can be obtained from experimental data of interaction with a silicon plate. We found specific surface energy of silicon applying well-known equation of point contact with adhesion

interaction  $P_{max}=2\pi R(\gamma_{probe}+\gamma_{sample})$ . Measuring the force  $P_{max}$ , at which two identical bodies are in a point contact, it is possible to calculate their specific surface energy. We calculated the specific surface energy of silicon to be equal  $0.0091 J/m^2$ .

Calculation of specific surface energy of tested samples was carried out at known specific surface energy of a silicon ball. The maximal force of attraction  $P_{max}$  and distance of attraction were determined from experimental data (Table 5). The table also includes calculated specific surface energy of tested samples. Calculated values  $\gamma$  for samples Si and Si+Epoxilane are very close to values, which are obtained at interaction of these samples with silicon ball. In contrary to these results, values  $\gamma$  for coatings  $Si+TiO_x+ODPO_4$  and  $Si+TiO_x$  are much different.

In Figure 6 we present the forces normalized by radius of indenter for contact adhesion meter (CAM) and AFM [6]. The data well concise excepting Ti and  $TiO_x$  samples. The difference can be explained by influence of capillary forces in adhesion meter comparing to AFM tip, capillary forces should play dominant role in the interaction of samples during retraction.

Another reason can be related to different kinematics of the instruments. In case of AFM we have a dynamic system while in CAM case it is quasi-static one.

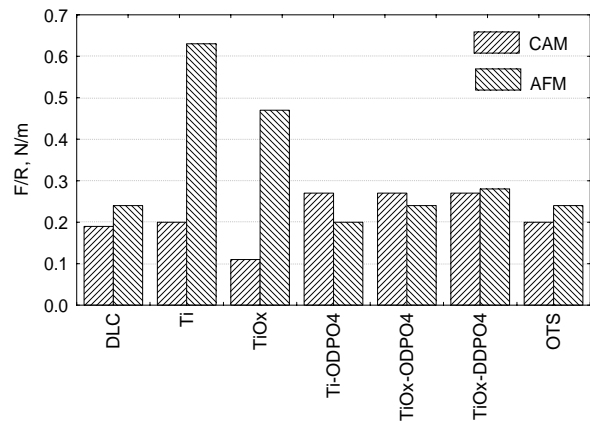


**Figure 6:** Adhesion (CAM) and pull-of forces (AFM) of the specimens.

**Table 5: Experimental and calculated characteristics of tested materials**

Specimens	Attraction force $P_{max}$ , $N \cdot 10^{-6}$	Distance $h$ , $m \cdot 10^{-9}$	Specific surface energy $\gamma$ , $J/m^2$
Test solid – silicon, radius of $1 \cdot 10^{-3}$ m			
Si	114	95	0.009
Si+Ti	34	124	0.004
Si+TiO <sub>x</sub>	143	111	0.014
Si+TiO <sub>x</sub> +ODPO <sub>4</sub>	99	91	0.007
Si+Ti+ODPO <sub>4</sub>	125	121	0.011
Si+Ti+DDPO <sub>4</sub>	67	115	0.002
Si+DLC	106	125	0.008
Si+epoxilane	33	92	0.004
Si+OTS	80	115	0.004
Test solid – titanium, radius of $1.5 \cdot 10^{-3}$ m			
Si	123	110	0.009
Si+epoxilane	38	51	0.003
Si+SEBS	12	50	0.002
Si+TiO <sub>x</sub> +ODPO <sub>4</sub>	34	14	0.004
Si+TiO <sub>x</sub>	28	33	0.002

### 3.2 Measurement of friction

Figure 7 shows the test results of the monomolecular coating SEBS deposited to the silicon substrate. A ball 3 mm in diameter made of steel 52100 (AISI) was used as a counterbody.

Simultaneously with the recording of the friction force the rate of counting AE pulses is recorded from the transducer output that is located under the plate specimen. It is seen that the rate of AE counting provides additional information on friction behavior of the system.

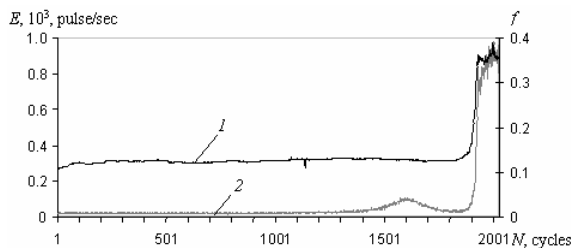


**Figure 7:** Friction coefficient  $f$  (1) and AE counting rate  $E$  (2) vs. number of test cycles  $N$ . Normal load  $P = 300$  mN; sliding velocity  $v = 4$  mm/s, track length  $S = 3$  mm

Table 6 presents data on friction coefficient of the investigated samples obtained with load 10 mN and sliding speed 0.5 mm/s.

**Table 6: Friction coefficients for test samples**

Coating	Thickness, nm	Friction coefficient	Number of cycles
Si	1.2	0.12	20 000
DDPO <sub>4</sub>	1.67	0.08	250
ODPO <sub>4</sub>	2.2	0.09	350
OTS	2.6	0.08	20 000
SEBS	8	0.09	20 000

## 4. CONCLUSIONS

The contact adhesion meter having a quasi-static operation mode can provide valuable data on force-distance behavior of solids at nanoscale distances. These data can be useful in addition to AFM and SFA data. The investigation of friction characteristics of miniature components, thin films and coatings makes necessary special testing conditions such as light loads, low sliding velocities and high sensitivity of friction force measuring systems. Mechanical noise of the motor system must be limited especially in case of acoustic measurements combined with tribotesting.

## 5. REFERENCES

- [1] Handbook of Micro/Nano Tribology. ed. Bh. Bhushan, CRC Press, New York, 1995
- [2] Sitti, M., Horiguchi, S., Hashimoto, H.: Tele-touch feed-back of surfaces at the micro/nano scale. Proc of IEEE/RSI Int. Conf. on Intelligent Robots and System, 1999, Korea
- [3] Deryagin, B.V., Krotova, N.A., Smilga, V.P.: Adhesion of Solids. Ed. Nauka, Moscow, 1973
- [4] J.N. Israelachvili: Intermolecular and Surface Forces, NY, 1991
- [5] Hofer R., Textor M., Spencer N.D.: Alkyl Phosphate Monolayers, Self-Assembled from Aqueous Solution onto Metal Oxide Surfaces. Langmuir, 17 (2001), 4014-4020
- [6] Myshkin, N.K. et al.: Interfacial Force and Friction Measurements of SAM-Coated Surfaces. Smart Surfaces in Tribology: Advanced Additives and Structured Coatings, 2003, Zurich, Switzerland